Canadian Mineralogist
Vol. 14, pp. 462-478 (1976)

AN EXPERIMENTAL STUDY ON THE SERPENTINIZATION OF IRON-BEARING OLIVINES

JUDITH B. MOODY
Department of Geology, University of North Carolina, Chapel Hill, N.C. 27514

Abstract

From bracketing experiments, the *P-T* curve, which defines the minimum thermal stability of olivine (Fo_{93}) for the assemblage olivine+chrysotile +brucite+magnetite+fluid, is shifted 15°C to lower temperatures for 0.5-2.0 kbar *P*(total) from the one defined by Johannes (1968) for the assemblage forsterite+brucite+chrysotile+fluid. Reversal has been demonstrated between major phases, but not in the exchange reactions ($Fe^{2+} \rightleftharpoons Mg^{2+}$) due to the sluggish nature of those reactions. The experimental results approximate very closely the observed phase assemblage in serpentinized dunites, suggesting that the reaction curve is a good indicator of the low-temperature stability of iron-bearing olivine in a hydrous environment.

Both lizardite and chrysotile were produced in the experiments with platy lizardite forming first, followed by fibrous chrysotile with increasing duration of the runs. Lizardite replaces olivine first, before chrysotile, due to the close topotactic relationship between the olivine and lizardite structures. Kinetically, the nucleation and growth of lizardite occurs with relative ease compared to chrysotile. Lizardite can be shown to be thermodynamically metastable compared to chrysotile because only one serpentine mineral can be in equilibrium with the other phases in the reaction investigated.

The iron content of the brucite (0-18 mole % $Fe(OH)_2$) was shown to be inversely related to the amount of magnetite produced in the bracketing experiments. The breakdown of ferrous hydroxide suggests that the brucite solid solutions are stable at lower temperatures compared to pure brucite and magnetite. Under low $f(O_2)$ conditions the iron content of olivine and the temperature at which serpentinization takes place control the amount of iron in the brucite.

Sommaire

D'après une série d'expériences en fourchette, la courbe *P-T*, qui définit la stabilité thermique minimale de l'olivine (Fo_{93}) dans l'association olivine +chrysotile+brucite+magnétite+liquide, se situe, pour une pression totale *P* de 0.5 à 2.0 kbar, à 15 degrés C sous la courbe définie par Johannes (1968) pour l'association forstérite+brucite+chrysotile+ liquide. Le renversement a été démontré entre les phases principales, mais non pendant les réactions d'échange ($Fe^{2+} \rightleftharpoons Mg^{2+}$) à cause de la lenteur de ces réactions. Les résultats expérimentaux sont très proches de ceux que donnerait l'association de phases des dunites serpentinisées; on peut donc supposer que la courbe de réaction est un bon indicateur de la stabilité de l'olivine ferrifère à basse température en milieu hydraté.

La lizardite et le chrysotile ont été produits pendant les expériences; la lizardite tabulaire se forme d'abord, le chrysotile fibreux vient ensuite lorsque l'expérience est de durée suffisante. La lizardite (avant le chrysotile) remplace l'olivine; ce remplacement est topotaxique. Cinétiquement parlant, la nucléation et la croissance se font plus facilement pour la lizardite que pour le chrysotile. Thermodynamiquement, la lizardite est métastable par rapport au chrysotile, parce que, dans la réaction étudiée, il ne peut y avoir qu'un seul minéral de serpentine en équilibre avec les autres phases.

La teneur en fer de la brucite (0-18% mol. $Fe(OH)_2$) est inversement proportionnelle à la quantité de magnétite produite pendant l'expérience. La décomposition de l'hydroxyde ferreux fait penser que les solutions solides de brucite sont plus stables, aux basses températures, que la brucite pure et la magnétite. Pour de faibles valeurs de $f(O_2)$, la teneur en fer de l'olivine et la température de serpentinisation régissent la quantité de fer dissous dans la brucite.

(Traduit par la Rédaction)

Introduction

Recent experimental and petrographic study of the retrograde metamorphism of dunites to produce serpentinites allows the following statements on the serpentinization process: (a) the dominant minerals produced are lizardite, chrysotile, ±brucite±magnetite, such that reaction (1) generally describes the hydration of many dunites (Johannes 1968):

$$\underset{\text{olivine}}{2Mg_2SiO_4} + 3H_2O = \underset{\text{chrysotile}}{Mg_3Si_2O_5(OH)_2} + \underset{\text{brucite}}{Mg(OH)_2} \quad (1);$$

(b) the presence of brucite means that the mineral assemblage of reaction (1) represents a lower *P,T* of serpentinization when compared to reaction (2) (Scarfe & Wyllie 1967; Chernosky 1973):

$$\underset{\text{talc}}{Mg_3Si_4O_{10}(OH)_2} + \underset{\text{forsterite}}{6Mg_2SiO_4} + 9H_2O = \underset{\text{chrysotile}}{5Mg_3Si_2O_5(OH)_2} \quad (2);$$

(c) the iron component of olivine is partitioned between serpentine and brucite, or forms a separate phase — magnetite (Mumpton & Thompson 1966; Hostetler *et al.* 1966; Johannes 1969); (d) the fluid involved in hydration more than likely has a complex origin: it becomes alkaline, is CO_2–poor, low in Mg and may have a high chloride content (Barnes & O'Neill (1969); Barnes *et al.* 1972); (e) the presence of silica-bearing, alkaline fluids changes the serpentine mineralogy and the serpentinization process as defined by reaction (1) (Korytkova & Markarova 1971; Korytkova *et al.* 1972), emphasizing the importance of fluid-mineral interaction; and (f) serpentinization takes place over a wide range of *T,P* conditions, i.e. from the earth's surface to some depth within the earth (Barnes & O'Neil 1969; Barnes *et al.* 1972).

Olivine in dunites typically varies between Fo_{95} to Fo_{80} with an average of Fo_{90} (Miyashiro 1966). With the development of oxygen buffer techniques (Eugster 1957, 1959; Eugster & Wones 1962) it has become possible to consider the effect of adding iron to the system MgO–SiO_2–H_2O. Such experiments obviously provide a closer simulation of the natural systems. The present work was undertaken: (1) to determine the effect of iron on the equilibrium curve defined by Johannes (1968) for the reaction involving brucite; (2) to evaluate the chemical parameters that affect the mobility of iron during the reaction, i.e., its partition among serpentine or brucite or the formation of magnetite; and (3) to determine by careful mineralogical analysis which factors influence the formation of the different serpentine minerals.

Experimental Methods

Hydrothermal runs

Charges were loaded into noble-metal capsules with a fluid phase as described by Huebner (1971), placed in cold-seal pressure vessels (Tuttle 1949), and subjected to a temperature-pressure regime for a given period of time. A double capsule was used: an inner Ag one contained a silicate charge + fluid and was crimped, but not welded, an outer Au capsule contained a buffer charge + fluid and was welded shut. The *P-T* fluctuations were within ±5°C and ±30 bars. The entire temperature measuring circuit was calibrated against the melting points of Zn (419°C) and Bi (271°C). The solids resulting from the quenched experimental runs were examined by optical, X-ray and SEM techniques to characterize their mineralogy and compositions.

Synthetic olivines, Fo_{88}, Fo_{95} and Fo_{100} (Table 1), were prepared hydrothermally from a mixture of MgO, SiO_2 and native iron according to the method of Fisher & Medaris (1969). The MgO was dried 48 hours at 115°C in a drying oven and stored in a vacuum desiccator. The SiO_2 was obtained as pure silica glass tubing (99.9%), crushed to 150 mesh, washed in weak HCl and then several times in water. Then, the silica was fired at 600°C and stored. As well, synthetic olivines were obtained from G. W. Fisher, Johns Hopkins University, (OP 194 and OP 54) and A. G. Plant, Geological Survey of Canada, (GSC olivine). Two natural olivines were supplied by R. G. Coleman, U. S. Geological Survey, (2-BU-66) and F. J. Wicks, Royal Ontario Museum, (M7863). Native iron for the buffer charge was added in the form of iron filings (99.999%) or as iron sponge (99.99%). A polished section of the iron sponge showed a small amount of magnetite (< 2%).

In the *hydration* experiments, the starting material was an olivine (synthetic or natural) plus a fluid phase (water, NaCl solution, etc.) The *equilibrium* runs (i.e. reversed or bracketing experiments) had an equal-weight mixture

TABLE 1. CELL PARAMETERS AND COMPOSITIONS OF OLIVINE STARTING MATERIALS

Olivine	a (Å)	b (Å)	c (Å)	V (Å^3)	d_{130}(Å)	composition mole % Fo*
2-33	4.758(2)	10.242(5)	5.996(3)	292.22(22)	2.7729	88
2-17	4.757(1)	10.213(1)	5.984(1)	290.73(4)	2.7683	95
2-19	4.754(1)	10.205(2)	5.983(1)	291.82(29)	2.7660	100
†GSC Fo(90)	4.758(1)	10.214(2)	5.989(1)	291.13(11)	2.7695	93
††OP194	4.770(1)	10.258(3)	6.009(2)	292.04(8)	2.7781	80
††OP54	4.813(1)	10.417(2)	6.067(1)	304.18(5)	2.8155	20
°M7863	4.764(1)	10.228(1)	5.994(1)	292.04(8)	2.7730	88
°°2-BU-66	4.759(1)	10.215(1)	5.988(1)	291.08(4)	2.7691	94

Parenthesized figures represent the estimated standard deviation (esd) calculated from Burham's (1962) program in terms of least units cited for the value of their immediate left, thus 4.758(2) indicates an esd of 0.002

*composition calculated from d(130) with determinative curve of Fisher & Medaris (1969), maximum error is ±2 mole % Fo

†synthetic olivine of composition 92.9 mole % Fo reported by Jambor & Smith (1964)

††synthetic olivines reported by Fisher & Medaris (1969), OP194 cell refinements were re-determined in this study

°natural olivine, Royal Ontario Museum M7863, Arizona, U.S.A.

°°natural olivine separate, Burro Mt., California, Loney *et al.* (1971, Table 4) reported 92.5 mole % Fo from a chemical analysis

of reactants and products plus water as the starting material. The equilibrium mix was made by reacting a synthetic olivine with water to give the products (Run 3-48) and then combining an equal weight of these products with the same olivine. This method differs from that used by Johannes (1968) and Chernosky (1973) who synthesized all phases of the reaction separately, then put them together in an equal-weight mixture. A few *dehydration* experiments were done in which the starting material consisted of the product phases (serpentine, brucite, magnetite, trace olivine) plus water placed in the pressure-temperature stability field of olivine+water.

Analysis of products

A Guinier-Hagg (IRD-Guinier XDC-700) powder pattern with Cu$K\alpha_1$ radiation (1.54051Å) was obtained on all starting materials and products with NaCl as an internal standard (calc. a_0 =5.6402Å). The X-ray patterns were read on a manual film reader to 0.01mm. All X-ray lines were corrected to the internal standard and then least-squares refinement was done using both Burnham (1962) (olivine & brucite) and Evans *et al.* (1963) (serpentine) programs. X-ray intensity measurements were attempted for determination of reaction direction in the reversed experiments. The films were measured with a double-beam recording microdensitometer. In relation to the starting material, a 20% change of the X-ray intensities of the completed run was observed before a reaction change was noted.

A polished section of the buffer charge was made following the method of Kullerud (1971) and examined in reflecting light. Grain mounts were made of the silicate products and examined in both transmitted and reflected light. Optical observation of the charge was essential in the identification of magnetite. Phase-contrast microscopy was useful in detecting small amounts of olivine and/or brucite.

The SEM was found to be very useful and in some cases essential in the documentation of run products. The sample was mounted on a small glass cover slip glued to sample holder and coated with C and AuPd before observation on the Cambridge Steroscan 600. Moody (1974) gives further details on the problems encountered with synthetic samples in SEM analyses.

R. B. Hargraves of Princeton University performed magnetic measurements on several starting materials and products to determine the net amount of magnetite produced during the reaction. The magnetic moment of a weighed sample was measured as a function of field strength on a Frantz translation balance. This was then related to the amount of magnetite in the sample.

Experimental Results

Oxygen fugacity

In view of the uncertainty involved in the effectiveness of the oxygen buffers below 500°C (Eugster & Wones 1962; Wise & Eugster 1964; Shaw 1967; Heubner 1971), an open inner capsule was used to ensure gas transport from the buffer charge to the inner silicate charge. The buffer charge was examined in polish section at end of each run to ascertain presence of both iron and magnetite. The oxygen fugacity at temperature and pressure of the experiment for IM buffer can be calculated from thermochemical data as outlined by Eugster & Wones (1962). Standard states for solids, liquids and gases are as defined in Robie & Waldbaum (1968). With more recent data sources (Table 2), the oxygen fugacity for buffer IM is defined by:

TABLE 2. REFERENCES FOR DATA USED IN CALCULATION OF GAS FUGACITIES

Data	Reference
$\Delta G^{o}_{f,M}(T)$	Haas & Robie (1973)
V_M	Robie & Waldbaum (1968)
V_{Fe}	Robie & Waldbaum (1968)
γH_2	Shaw & Wones (1964)
γH_2O	Burnham *et al.* (1969)
K_w	Zen (1973)

$$\log f(O_2) = -28880/T + 8.240 + [0.0607(P-1)]/T \quad (3)$$

Figure 1 illustrates the variation of gas composition as a function of temperature and total pressure for IM buffer and for the assemblage magnetite–awaruite (Ni_3Fe and Ni_2Fe). M-A is important in defining the $f(O_2)$ conditions in serpentinized ultramafic rocks where it is a common assemblage. Thermochemical data for awaruite were obtained from Kubaschewski & Goldbeck (1949) and $f(O_2)$ was calculated in the same manner as for IM buffer.

Hydrothermal runs on the reaction of olivine with an aqueous fluid

The starting materials were characterized by optical and X-ray studies (Table 1). Small amounts of impurities, mainly magnetite, were observed in olivine 2-17 (< 3%) and reported in OP 194 and OP 54 (Fisher & Medaris 1969). Both natural olivines were single phase and unzoned from X-ray and optical examination.

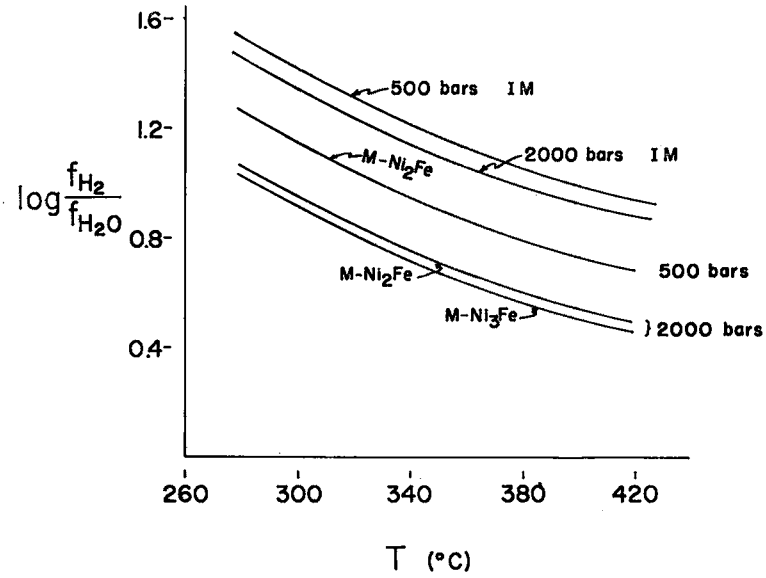

FIG. 1. Log $f(H_2)/f(H_2O)$ vs. temperature for the assemblages iron-magnetite (IM), magnetite-awaruite (Ni_2Fe-Fe_3O_4 and Ni_3Fe-Fe_3O_4) for P_{total}=500 and 2000 bars. Calculations are described in text. At 500 bars, the difference between the log $f(H_2)/f(H_2O)$ for M-Ni_2Fe and M-Ni_3Fe is too small to be meaningful within the error of the thermodynamic data and assumptions necessary for the calculations.

Details of the starting material, temperature, pressure, run duration, and product phases for the hydrothermal runs are given in Appendix 1. Each major phase is considered in light of the experimental as well as the optical, X-ray and SEM data. The term "hydration" run is used to define a type of reaction that chiefly involves the addition of water (Martin & Fyfe 1970; Fyfe 1973) and is therefore a reaction studied in one direction only.

Olivine

The iron content of olivine was determined in order to aid in evaluating the mobility of iron during the alteration process. A small change in composition was observed for some of the olivines which persisted metastably outside their stability field.

Olivine appeared in the SEM as anhedral massive grains, ranging in size from 20 to 100 μm. The alteration of olivine was very sluggish in pure water and sodium chloride, but relatively rapid in the various alkaline fluids. As is usually the case, the finer grained synthetic olivines were more reactive than the natural olivines. No other difference between the natural and synthetic olivines was noted.

Serpentine minerals

Lizardite has not been reported previously as a reaction product in an experimental study on determination of olivine's thermal stability, though it is a common serpentine mineral in natural serpentinites. Johannes (1968) used chrysotile as the serpentine component in the starting mixture for the equilibrium determination of the brucite reaction (Equation 1) as did Chernosky (1973) for the equilibrium determination of the higher temperature talc reaction (Equation 2). Scarfe & Wyllie (1967) did not identify the serpentine mineral formed in their experiments.

Both lizardite and chrysotile were produced in the present experiments. Detection of the first appearance of lizardite was not difficult optically or in the Guinier X-ray powder pattern. However, detection of chrysotile in a mixture of olivine+lizardite was difficult due to overlapping diffraction lines and lack of positive optical identification due to fine grain size of serpentine. The SEM was extremely useful in solving this problem and allowed easy detection of chrysotile due to its distinctive fibrous habit. For example, in Run 3-30, olivine and lizardite were detected in an X-ray pattern, brucite and magnetite optically, and chrysotile by SEM.

Lizardite was refined on the basis of an orthorhombic cell (Table 3). The largest variations in cell dimensions were for lizardite formed during the reaction of olivine with water and fluids of varying composition compared

TABLE 3. LIZARDITE CELL PARAMETERS

Run	a(Å)	b(Å)	c(Å)	V(Å^3)	d_{002}(Å)†
3-99	5.295(1)*	9.174(2)	7.310(1)	355.1(1)	3.655
3-76	5.322(1)	9.196(2)	7.292(3)	356.9(1)	3.649
3-75	5.306(7)	9.201(3)	7.301(6)	356.5(3)	3.652
3-74	5.315(9)	9.190(9)	7.290(19)	356.1(9)	3.656
3-72	5.299(3)	9.187(2)	7.301(2)	355.4(1)	3.650
3-71	5.302(18)	9.199(5)	7.300(15)	356.0(8)	3.649
3-78	5.317(7)	9.187(8)	7.290(15)	356.1(8)	3.651
3-70	5.318(3)	9.190(5)	7.300(7)	356.7(4)	3.653
3-97	5.315(5)	9.199(5)	7.300(11)	356.9(5)	3.655
3-68	5.301(3)	9.176(1)	7.314(3)	355.8(1)	3.656
3-69	5.317(8)	9.195(8)	7.300(16)	356.9(8)	3.656
3-47(L)	5.317(5)	9.198(6)	7.280(11)	356.1(5)	
3-77(L)	5.302(10)	9.199(3)	7.310(3)	356.6(4)	3.656
**241M(L)	5.312(4)	9.204(17)	7.237(15)	353.8(11)	3.619
°M19804 (L)	5.319(2)	9.223(3)	7.313(6)	358.8(2)	3.661
°°M19142 (L)	5.317(1)	9.208(2)	7.305(4)	357.6(2)	3.653

†d(002)-observed basal spacing of serpentine minerals. Chernosky (1975) showed maximum variation in Al content to be reflected in d(002) of serpentine; Forbes (1969) illustrated change in iron content of talc with its basal spacing

*figures in parentheses represent the estimated standard deviation (esd) calculated from the Appleman *et al.* (1963) program, 5.318(3) indicates an esd of 0.003.

**synthetic lizardite and chrysotile (Chernosky 1975)

°natural lizardite 1*T*, Royal Ontario Museum, M19804, Madoc Tp., Ontario

°°natural lizardite 1*T*, Royal Ontario Museum, M19142, Dypingdal, Snarum, Norway

TABLE 4. VARIATION IN LIZARDITE CELL DIMENSIONS

	Hydration Runs*	Δ	Bracketing runs**	Δ
a (Å)	5.278 - 5.380	0.102		0.013
b	9.143 - 9.211	0.068		0.022
c	7.290 - 7.329	0.039		0.018
V (Å^3)	355.08 - 361.73	6.65		0.68

*individual X-ray data provided on request.

**X-ray data given in Table 3.

to those lizardites from the bracketing experiments (Table 4). No systematic variation was found in cell dimensions or volume with temperature and pressure of formation or with composition of initial starting olivine. The reduction in variation of the cell parameters (as noted above) and formation of euhedral lizardite crystals in bracketing and dehydration experiments is due to increased run duration, which allows the lizardite to achieve better crystallinity and become structurally more perfect with time (Ross 1968; Forbes 1969).

Appendix 2a presents a few X-ray diffraction patterns for the synthetic lizardites produced in this study. Comparison of X-ray data for massive, platy lizardite (3-61, 3-4) versus euhedral lizardite (3-97, 3-76) shows that there are a larger number of powder diffraction lines and better agreement between d_{calc} and d_{obs} for euhedral lizardites. The lizardite polytype is very difficult to determine because about 50% of the lizardite lines also coincide with lines of olivine or brucite. Therefore, the calculated X-ray intensities for polytypes (Bailey 1969) cannot be used to distinguish the difference between lizardite 1*T* or 2*H* (Wicks & Whittaker 1975). However, the X-ray pattern for lizardite M19804, identified as 1*T* by Wicks (pers. comm. 1975), coincides very closely with the observed lizardite patterns. Only the weaker (200) and (202) reflections are consistently missing from the X-ray patterns for the synthetic lizardites in comparison to lizardite M19804.

Whittaker & Zussman (1956) established that c=14.6Å for clinochrysotile. Yada (1967, 1971) has presented evidence from lattice fringe edge dislocations that the repeat unit in the c-direction also may be 7.3Å. Zvyagin (1967) has shown that both one-layer (7.3Å) and two-layer (14.6Å) monoclinic structure exists for chrysotile, but the one-layer structure has been identified only by electron diffraction patterns from single fibers. Wicks & Whittaker (1975) have demonstrated from polytypic considerations of the serpentine minerals that both one- and two-layer monoclinic structures are permissible stacking sequences for chrysotile (e.g. polytype $2M_{cl}$ and $1M_{cl}$). Where chrysotile makes up greater than 50% of the serpentine, the Guinier powder patterns allowed refinement of both chrysotile and lizardite cell dimensions (Table 5). Chrysotile gave poor refinements in most cases. These poor results are due to the small number of lines available for the refinement and the varying degree of fiber development in the synthetic samples. Comparison of the synthetic chrysotile X-ray diffraction lines (Appendix 2b) with the chrysotile M8507 pattern, identified as $2M_{cl}$ (F. J. Wicks, pers. comm. 1975), shows close agreement, indicating that the synthetic samples are most probably $2M_{cl}$ polytypes. The $2M_{cl}$ is also the most common polytype of chrysotile (Wicks & Whittaker 1975).

TABLE 5. CHRYSOTILE CELL EDGE AND VOLUME DATA

Run	a(Å)	b(Å)	c(Å)	V(Å^3)	β
3-48	5.277(27)	9.214(7)	14.618(75)	703.8(6)	91° 57'(33')
3-22	5.269(16)	9.210(7)	14.650(74)	712.7(3)	93° 11'(11')
3-42	5.307(11)	9.213(11)	14.644(100)	715.1(4)	92° 53'(16')
3-64	5.305(6)	9.201(6)	14.622(54)	712.9(2)	92° 54'(8')
3-105	5.377(14)	9.213(7)	14.677(65)	719.9(36)	94° 5'(20')
*241M	5.306(6)	9.176(12)	14.650(8)	712.1(17)	93° 20'
**M8507	5.320(3)	9.208(4)	14.631(17)	715.72(8)	93° 18'

*synthetic chrysotile (Chernosky 1975)

**natural crysotile $2M_{cl}$, Royal Ontario Museum, M8504, Montreal Chrome Pit, East Broughton, Quebec.

The relationship between cell edge and chemical composition of the serpentine minerals is important in this study with respect to possible iron-for-magnesium substitution. Examination

of the scant data available in literature on lizardite cell parameters as a function of composition showed no correlation with respect to iron content. Direct analysis by microprobe of the serpentine produced in this study was considered, but the fine grain size of the minerals, coupled with problems of disaggregation of the intimate mixture of phases, discouraged attempts (see also Cameron 1975). An SEM with an energy dispersive accessory was not available for the study.

The common habits of the experimentally produced serpentine minerals from the SEM observations were: (1) massive, platy lizardite with or without crystal faces, (2) lizardite laths, (3) chrysotile fibers, (4) chrysotile fiber bundles in the longer runs within the serpentine stability field, and (5) small serpentine laths, which are probably lizardite, but have not been positively identified. The SEM data of the serpentine mineral habits correlate well with those observed from TEM and optical studies (Table 6). However, lizardite laths and euhedral, pseudohexagonal crystals have not been previously described in the literature. F. J. Wicks (pers. comm. 1974) has observed lizardite laths in his SEM studies of natural serpentine minerals.

The following were also noted from the SEM observations of the serpentine minerals in these experiments:

(1) laths of lizardite form at temperatures above 315°C at all pressures investigated and persist in runs up to 2500 hours in duration;
(2) euhedral, pseudohexagonal crystals of lizardite existed at temperatures less than 345°C at all pressures with run durations greater than 1100 hours, except in the sodium metasilicate fluid experiments where euhedral lizardite formed after only 573 hours;
(3) small serpentine laths (<3 μm in wdith) formed at lower temperatures (<310°C) at all pressures but did not persist with longer run durations (>1660 hours) except at the lowest pressure of 0.5 kbar;
(4) the alkaline chloride solution promotes growth of chrysotile rather than lizardite (Table 7).

TABLE 6. HABIT OF LIZARDITE AND CHRYSOTILE FROM TEM AND OPTICAL STUDIES

Mineral	Habit	Size (μm)†	Reference
lizardite	plates	50*	Zussman *et al.*(1957)
lizardite	plates	0.1-1.0	Iishi & Saito (1973)
lizardite	hexagonal plates	100-400	Krstanovic (1968)
lizardite	anhedral grains	1.0*	Zussman *et al.* (1957)
chrysotile	fibers	0.026	Whittaker (1957)
chrysotile	fibers	0.032-0.04	Kheiker *et al.*(1967)
chrysotile	fibers	0.018-0.2**	Yada (1967, 1971)
chrysotile	fibers	0.02***	Iishi & Saito (1973)
chrysotile	laths	0.2 maximum	Zussman *et al.*(1957)

†for chrysotile fibers, the outer diameter of fiber
*estimated from published photographs
**statistically significant, an average of 170 measurements of individual fibers on natural chrysotile from 5 different localities and one one synthetic chrysotile
***length 0.04-0.8 μm
For lizardite anhedral grains, read <1.0*.

TABLE 7. SEM RESULTS ON THE HABIT OF SERPENTINE AS A FUNCTION OF FLUID COMPOSITION

Run	T °C	P kbar	Run Duration	Fluid	Massive Platy L	Euhed- ral L	Fibers C	amt.*
3-42	306	0.99	573 hrs.	0.06 *M* NaSi†	x	x	x	L=C
3-52	302	1.00	550 hrs.	0.01 *M* NaOH	x		x	L>C
3-64	302	1.00	524 hrs.	0.33 *M* NaCl 0.02 *M* NaOH	x		x	C>L

*relative amount estimated visually from SEM samples

†sodium matasilicate, $Na_2SiO_3.9H_2O$

Thus, temperature may control the formation of lizardite laths, but not necessarily any of the other habits within the stability field of serpentine. The properties and composition of the fluid involved in the alteration of olivine may also influence the formation and habit of a given serpentine mineral.

Brucite and magnetite

Brucite occurred in all run products in which reaction had proceeded to such an extent that less than 60% of the olivine remained. Brucite was identifiable optically and by the SEM as euhedral, hexagonal platelets from 4 to 100

TABLE 8. IRON CONTENT OF OLIVINE AND BRUCITE WITH RESPECT TO MAGNETITE PRODUCTION

Run	T(°C)	P(kbar)	Mole % Fa*	Δ**	Mole % $Fe(OH)_2$***	Δ†	Amount of magnetite††
3-99	361	2.01	7	0	6(1)	+2	major
3-76	344	2.01	11°°	-4	11(1)	-3	minor
3-74	341	1.48	5°°	+2	9(9)	-1	minor
3-72	332	1.48	7°°	0	11(1)	-3	minor
3-84	341	1.01	2	+5	4(4)	+4	major
3-71	330	1.00	5°°	+2	2(2)	+6	major
3-78	321	1.01			15(9)	-7	minor
3-70	322	1.00			13(1)	-5	major
3-97	336	0.54	7	0	7(2)	+1	major
3-68	322	0.56			0	+8	major
3-25	323	1.94	7	-2	2(2)		trace
3-12	321	1.99			7(7)		trace
3-61	302	1.93			18(1)		major
3-48	309	1.48			8(1)		major
3-1	302	1.01			10(1)		major
3-4	317	1.01			5(2)		major
3-22	304	0.54			6(2)		major
3-105	355	2.01	12°°	-5	7(2)		major
3-103	355	1.01	9°°	-2	5(5)		major
3-104	330	1.01	16°°	-9	6(2)		major

*composition of olivine at end of run, mole % fayalite
**change in the composition of olivine from the starting material
***mole % $Fe(OH)_2$ determined from d_{001} (c cell edge) after Mumpton & Thompson (1966), error calculated from eds in c cell-edge refinement; Page (1966) has shown good agreement between iron content of brucite and X-ray cell-edge determination and electron microprobe analysis of brucite
†change in composition of brucite from the starting material
††estimation from optical observation of charge
°°trace amounts of olivine remaining at the end of the run

μm (Fig. 3B). The iron content of brucite was determined from X-ray cell edge data and varied between 0-18 mole % $Fe(OH)_2$. Table 8 collates all the data on iron contents of phases and the production of magnetite. These data indicate: (1) at constant pressure, the higher the temperature the greater the amount of magnetite produced; (2) the greater magnetite production correlates with lower iron content of coexisting olivine and brucite; (3) brucite has the highest iron content in the lowest temperature runs for the bracketing experiments at each pressure; and (4) in longer-duration hydration experiments small variations in iron content of brucite (5-10 mole % $Fe(OH)_2$) can be correlated with major amounts of magnetite formed (Runs 3-48, 3-1, 3-4, and 3-22).

The iron content of brucites from partly and completely serpentinized ultramafic rocks are summarized in Table 9. Wicks (1969) noted

TABLE 9. IRON CONTENT OF BRUCITE WITH COEXISTING MAGNETITE FROM SERPENTINIZED DUNITES

Serpentinite	mole % Fa*	% Serpentinized	Serpentine Mineralogy	Average Brucite mole % $Fe(OH)_2$
Dun Mountain,[1] New Zealand	8.5	58	L, minor C	16 (10.5-19.0)†
Hat Island,[1] Wash.	6.0	98	L, minor C	16.5 (5.9-24.7)
New Idria,[1],[2] Calif.		100	L + C	15 (11.4-17.7)
Twin Sisters,[1] Wash.	9.0	56	L	14 (11.4-16.0)
Burro Mtn.,[1],[3] Calif.	7.5	54	L	13 (10.5-18.2)
				18-32
				(0-50)
Mount Albert,[4] Quebec	8-10	70	L	6-12
				(6-42)
Muskox,[4] N.W.T.	15-20	70	L	60-70

*original composition of olivine, mole % fayalite

†numbers in parenthesis indicate the range of values found for brucite compositions

(1) Hostetler *et al.* (1966), brucite composition determined by microprobe and chemical analysis

(2)Mumpton & Thompson (1966) X-ray determination

(3)Page (1967), X-ray and microprobe analysis

(4)Wicks (1969), X-ray analysis

that the absence of magnetite in some serpentinized dunites may be related to the production of an iron-rich brucite (e.g. Mayaguez Intrusion, Puerto Rico; Glen Urquhart Intrusion, Scotland). However, Wicks (1969), Hostetler *et al.* (1966) and Page (1967) have observed iron-bearing brucite coexisting with magnetite. Wicks suggested that the iron content of brucite may be related to the original iron content of the olivine (see Table 8); e.g., in the original dunite of the Muskox Intrusion, the olivine was iron-rich and then produced an iron-rich brucite upon serpentinization. Because the iron content of the brucite depends on the original composition of the olivine, it provides an explanation for the limited range of iron content of the synthesized brucites: they reflect the limited compositional range of the original olivines.

Magnetite was identified optically in all run products as either fine micron-size particles (1-2 μm, "dusty") or as larger grains (4-10 μm). When the grain size and amount of magnetite became large enough it could be identified in the X-ray pattern. Besides longer run duration at a given temperature and pressure (Runs 3-32 and 3-48), higher temperatures promote formation of larger grains of magnetite and euhedral crystal forms. Table 10

TABLE 10. MAGNETIC MEASUREMENTS* OF SELECTED STARTING MATERIALS AND RUN PRODUCTS

Material	Js emu/g	Eq. M wt. %	Net Increase M, wt, % **
M7863†	0.03	0.04	
equil mix††	0.23	0.25	
2-98	4.5	4.8	4.8°
2-100	0.68	0.70	0.66
3-71	3.3	3.5	3.25
3-84	8.85	9.5(5)°°	9.25
3-76	0.64	0.69(1)°°	0.44

* courtesy of R.B. Hargraves, Princeton University

** net increase in amount of magnetite: product magnetite minus the magnetite in starting material

† starting material for Run 2-100

†† starting material for Runs 3-71, 3-84, 3-76

° a magnetic measurement was not made of the starting material; however, magnetite was not observed in starting material with optical and X-ray examination

°°average of two measurements, esd calculated from error in measurement

presents several magnetic measurements, which reflect the amount of magnetite in the sample. More magnetite was produced in Run 2-98 than in 2-100. Those runs differ in temperature (2-98, lower of the two) and starting material but are otherwise identical. Run 2-98 had a synthetic olivine as starting material, and 2-100 had a natural olivine of which approximately 70% remained at the end of the run. The incompleteness of the reaction for Run 2-100 accounts for the lower magnetite production in comparison to Run 2-98. The magnetic measurements of the bracketing experiments give further evidence for the increased amount of magnetite with increased temperature (Runs 3-84 and 3-71). Considering the optical observations in Table 8, Run 3-99 produced more magnetite than the 0.69 wt. % observed for Run 3-76, following the increased temperature trend for a given pressure.

Phase Relationships

Influence of iron on thermal stability of olivine

In order to establish criteria of equilibrium,

it was necessary to study the reaction of an iron-bearing olivine with water in both directions, i.e., to conduct bracketing experiments. The criteria developed for determining the mineral stability fields from the habit of the phases as observed by the SEM are illustrated in Figures 2, 3 and 4. Table 11 compares the results from the microdensitometer intensity measurements of the Guinier X-ray powder diffraction patterns and SEM results. The intensity measurements give information on the relative amounts of phases present whereas the SEM observations illustrate features of growth and dissolution. The SEM data (for Runs 3-97, 3-98, 3-85, 3-87, 3-86, 3-99, 3-100) were clearly definitive in determination of reaction direction where the X-ray intensity measurements were not. Conflict between the two sets of observations was observed in Run 3-98 at lowest pressure (0.5 kbar) near the boundary curve, where reaction rate is the most sluggish. In Run 3-86 the amount of water was very large compared to the amount of equilibrium mix; the X-ray data

TABLE 11. MICRODENSITOMETER INTENSITY MEASUREMENTS AND SEM° RESULTS FOR THE BRACKETING EXPERIMENTS

0.5 kbar

	3-69	3-68	3-97	3-98
Olivine	-(-)	-	-(-)	*(+)
Lizardite	*(*)	*	*	(-)
Chrysotile	*(*)	*	+(+)	+(-)
Brucite	*(+)	*	+(+)	+(-)
T (°C)	311	322	336	352
duration, hrs.	895	863	814	814

1.0 kbar

	3-70	3-71	3-84	3-85	3-87	3-86
O	-(-)	-(-)	-(-)	*(+)	+(+)	-(+)
L	*(+)	+(+)	*	*(-)	*(-)	-(-)
C	*(+)?	*(*)	+(+)	*(-)	*(-)	-(-)
B	*(+)	+(+)	*(*)	*(-)	*(-)	-(-)
T (°C)	322	330	341	349	361	371
duration, hrs.	837	792	568	567	568	569

2.0 kbar

	3-75	3-76	3-99	3-100	3-101
O	-(-)	-(-)	*(-)	*(+)	+(+)
L	*(*)	*(+)	*(-)	*(-)	-(-)
C	*(*)	+(+)	+(+)	*(-)	-(-)
B	*(*)	*(+)	+(+)	*(-)	-(-)
T (°C)	335	344	361	376	392
duration, hrs.	480	479	739	794	695

- disappearance of a phase °SEM results are in parenthesis
+ growth of a phase
* no change

For chrysotile 3-69, read *(+).

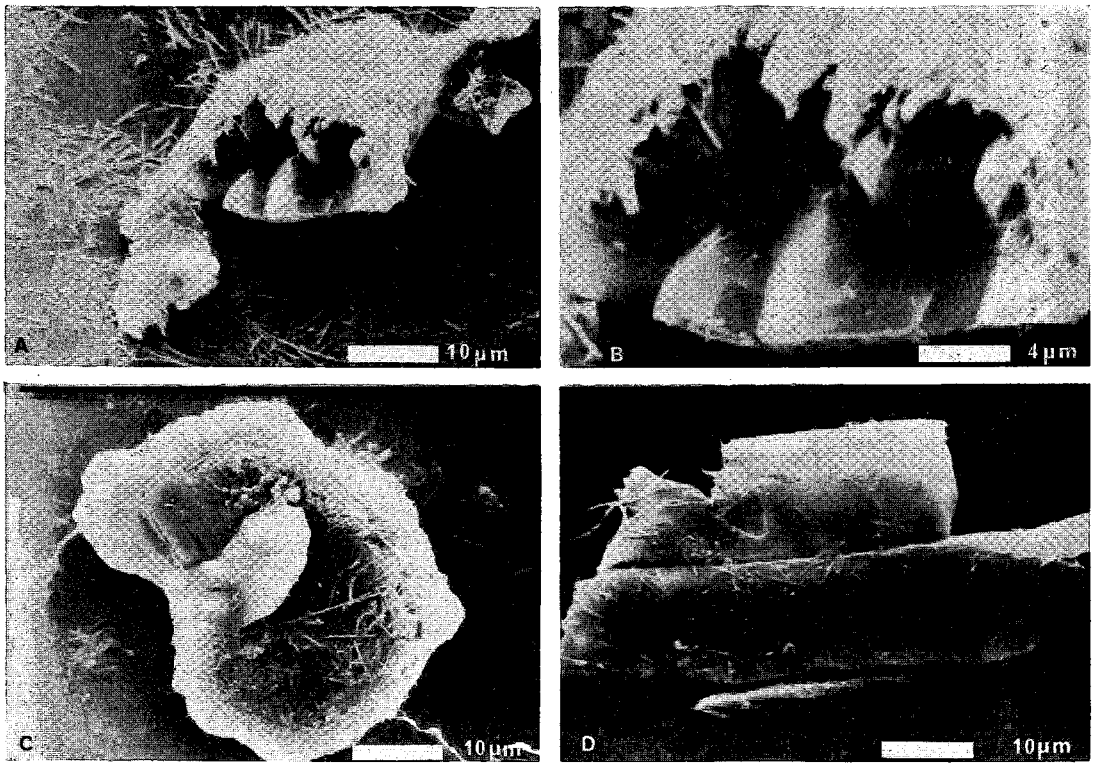

FIG. 2. Scanning electron microphotographs: (A) euhedral, stubby lizardite crystals with a coating of chrysotile fibers (Run 3-76, L+C+B+M stability field); (B) euhedral lizardite, higher magnification of Figure 2A (Run 3-76); (C) large euhedral lizardite plate, appears to be a substrate for chrysotile fibers (Run 3-75, L+C+B+M stability field); (D) lizardite laths, length about 60 µm (Run 3-99, L+C+B+M stability field).

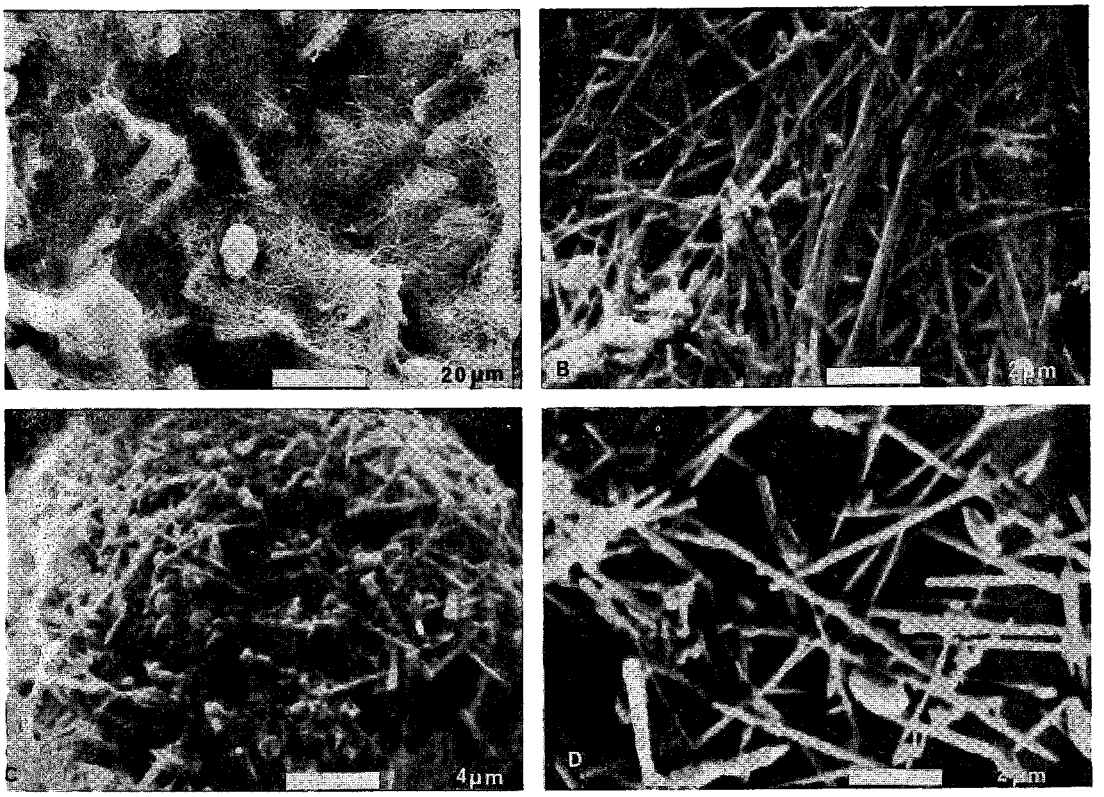

FIG. 3. Scanning electron microphotographs: (A) very short chrysotile fibers at early stages of development (Run 3-75); (B) lizardite lath, chrysotile fibers, and brucite platelets. The white area around the edge of the hexagonal brucite platelets is due to charging (Run 3-71, L+C+B+M stability field); (C) lengthening of chrysotile fibers as temperature is increased, compare to Figure 3A, conducted at a lower temperature (Run 3-76); (D) maximum development of chrysotile into fiber bundles up to 100 μm in length (Run 3-76).

indicate some dissolution of the total sample, though the SEM observations showed development of euhedral olivine crystals which are interpreted as growth features (as illustrated in Figs. 4C and 4D for Run 101).

Chrysotile replacement of lizardite is suggested by the SEM observations of the experiments of longer duration at higher temperatures. It is only in those runs that chrysotile fiber bundles developed and the amount of chrysotile was visually estimated to be equal to or greater than lizardite (Table 11, Runs 3-99, 3-84). Phase-rule considerations indicate that only one serpentine mineral can be stable in the system, leading to the conclusion that is implied above by experiment, i.e., lizardite is probably metastable with respect to chrysotile. The system may be described by these five components: MgO-FeO-SiO_2-H_2O-H_2. The phases observed along the boundary curve are: lizardite, chrysotile, brucite, magnetite, olivine and fluid. The phase-rule solution then indicates one degree of freedom. However, oxygen fugacity is an intensive variable so the boundary curve is in divariant, not univariant equilibrium. Five phases can coexist in divariant equilibrium and one can conclude that chrysotile (not chrysotile +lizardite) is the stable serpentine phase in the assemblage.

Figure 5 presents the T,P reaction boundary defined by the X-ray and SEM work. A mass-balance equation for the reaction can be written:

$$10(Mg_{1.86}Fe_{0.14})SiO_4+14.2H_2O = 5Mg_3Si_2O_5+(OH)_4+3.8(Mg_{0.95}Fe_{0.05})(OH)_2+0.4Fe_3O_4+0.4H_2.$$

The mixed solid solution can also be expressed ideally in terms of two independent end-member reactions:

$$5Mg_2SiO_4+Fe_2SiO_4+9H_2O = 3Mg_3Si_2O_5(OH)_4+Mg(OH)_2+2Fe(OH)_2 \quad (5)$$

$$3Fe(OH)_2 = Fe_3O_4+2H_2O+H_2 \quad (6)$$

The reaction boundary as investigated involves: (1) reversal between major phases in reaction,

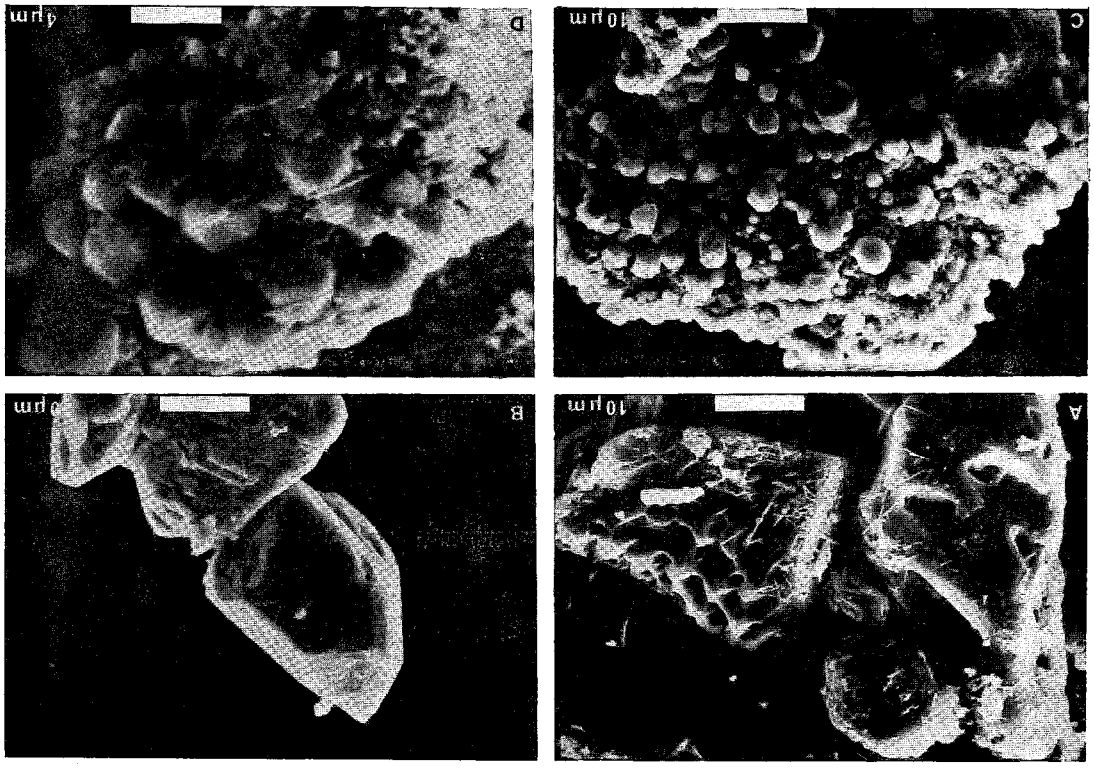

FIG. 4. Scanning electron microphotographs: **(A) etch** and solution pits in lizardite (Run 3-100, **O stability** field; (B) development of euhedral olivine crystals from the former angular grains (Run 3-101, O stability field); (C) euhedral olivine crystals developing on a pre-existing lizardite (?) substrate (Run 3-101); (D) small euhedral olivine crystals, similar to Figure 4C (Run 3-101).

i.e., equilibrium among minerals, (2) chemical equilibrium in iron distribution defined by the exchange reactions: $Fe^{2+}=Mg^{2+}$, and (3) oxidation-reduction (Reaction 6) which is a function of $f(O_2)$. Due to the sluggish nature of the reaction, true equilibrium was not demonstrated experimentally, particularly with respect to iron distribution among the phases, e.g. should brucite in Reaction 4 be pure $Mg(OH)_2$? The equilibrium assemblage along the boundary curve is chrysotile-brucite-magnetite-olivine-fluid. That equilibrium is suggested but *not* proven by experiment.

The 15°C shift to lower temperatures at all pressures when compared to the Johannes (1968) curve for pure forsterite is consistent with results obtained in other magnesium-iron systems (Forbes 1971). The curve is a good indicator of the minimum temperature of stability of iron-bearing olivines found in peridotites. The experimental results closely approximate petrologic observations of serpentinized dunites, suggesting that the formation of lizardite serpentinites may be a metastable process.

Stability of $Fe(OH)_2$

The stability of the brucite solid solution compared to its breakdown products (pure brucite, magnetite, water and hydrogen) is analogous to the annite-phlogopite stability reactions as determined by Eugster & Wones (1962) and Wones & Eugster (1965). Reaction (6) defines the breakdown of pure ferrous hydroxide and the equilibrium constant for that reaction is given by:

$$K_6 = [a_{Fe_3O_4} (a_{H_2O})^2 a_{H_2}]/(a_{Fe(OH)_2})^3$$

Because magnetite occurs as a pure phase, the equilibrium constant becomes:

$$K_6 = [(f_{H_2O})^2 f_{H_2}] / (a_{Fe(OH)_2})^3$$

The activity of ferrous hydroxide in the solid solution can be defined as:

$$a[_{Fe(OH)_2}] = [(f_{H_2O})^2 f_{H_2}]^{1/3}/[(f^*_{H_2O})^2 f^*_{H_2}]^{1/3}$$

where $f(H_2O)$ and $f(H_2)$ are the fugacities of hydrogen and water in equilibrium with the brucite solid solution and $f^*(H_2O)$ and $f^*(H_2)$ are the fugacities of hydrogen and water in

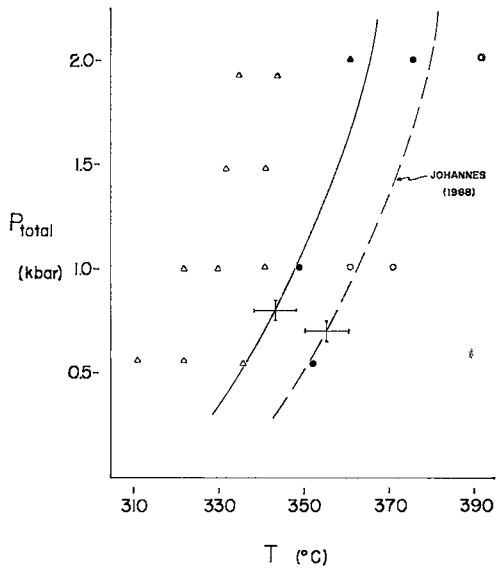

FIG. 5. The reaction curve for $10(Mg_{1.86}Fe_{0.14})SiO_4 + 14.2H_2O = 5Mg_3Si_2O_5(OH)_4 + 3.8(Mg_{0.95}Fe_{0.05})(OH)_2 + 0.4Fe_3O_4 + 0.4H_2$ determined with IM buffer. The open triangles indicate that olivine disappeared and the other phases grew, the open circles indicate that olivine grew and the other phases disappeared. The filled circles and triangles indicate the same direction of reaction as the open triangle or circles, but the direction of the reaction was determined from SEM results rather than X-ray intensity measurements (see Table 11). The dashed curve was determined by Johannes (1968) for the reaction: $2Mg_2SiO_4 + 3H_2O = Mg_3Si_2O_5(OH)_4 + Mg(OH)_2$. The error bars estimated by the authors are placed on the curves.

equilibrium with the pure ferrous hydroxide at the same temperature and P_{total}. The difference between this formulation and that of Page (1966, 1967) is that the brucite solid solution is defined here as a single phase consisting of two components, or — $Mg(OH)_2$ and $Fe(OH)_2$ —, and only one component need be considered thermodynamically to define the solid solution. However, from Page's treatment and considerations given above, the effect of increasing the $Mg(OH)_2$ component of the solid solution is to decrease the activity of $Fe(OH)_2$. Also, the thermal stability of end-member component $Mg(OH)_2$ is much greater than $Fe(OH)_2$. Therefore, for the same values $f(H_2O)$ and $f(H_2)$, the assemblage Mg-rich brucite+magnetite is stabilized relative to the iron-rich brucite at higher temperatures.

The general trend for the iron content of brucite in the experimental results may be explained. A correlation exists between the amount of magnetite produced and the iron content of brucite: a smaller amount of magnetite is associated with more iron in brucite; furthermore, the amount of magnetite increases with increasing temperature. These observations fit the experimental results and thermodynamic arguments on the stability of the brucite solid solution with respect to brucite+magnetite: Runs 3-76, 3-72, and 3-78 of the bracketing experiments had a higher iron content in brucite and less magnetite than Runs 3-99, 3-74, and 3-84, which were held at higher temperatures for each pressure and had more magnetite and less iron in the brucite. The iron content of the brucite may not only be an indication of the initial iron content of the olivine, but also an indication of the temperature at which serpentinization took place.

Martin & Fyfe (1970) reported that they did not observe the formation of magnetite in unbuffered experiments with a natural olivine (Fo_{85}) in the temperature range 200-300°C at 1.39 kbar and their X-ray cell-edge data on brucite suggest that iron entered the brucite structure. Martin & Fyfe's experiments were done to determine the temperature of the maximum rate of reaction of olivine+water; they were conducted 50-75°C lower than those done in this study. The lack of production of magnetite follows the trend reported here.

The iron content of brucites formed during experiments with NaOH fluids follows the same trend as defined in the runs with olivine+water; the lower the temperature, the more iron-rich the brucite. No iron was found in the brucites formed from the reaction of olivine with alkaline chloride solutions (Runs 3-95, 3-92), most probably due to the solubility of ferrous iron in chloride solutions by the formation of a ferrous chloride complex.

T,P, and composition effects on formation of serpentine

Figure 6 summarizes all known serpentine synthesis data and equilibrium phase boundaries determined for the serpentine minerals. The synthesis temperatures and pressures clearly bear no relationship to the determined phase boundaries for the reactions of interest. Iishi & Saito's (1973) work demonstrates that Al or Fe are not necessary for the formation of lizardite. The *T,P* fields of lizardite, chrysotile and antigorite determined by Iishi & Saito for a fixed $Mg(OH)_2$:SiO_2:H_2O reflect disequilibrium relationships, not surprising for runs lasting only five days. Also, Chernosky (1975) produced lizardite and chrysotile from an oxide mix (241M), where $x=0$ for $(Mg_{6-x}Al_x)(Si_{4-x}Al_x)O_{10}(OH)_8$. The data available on serpentine min-

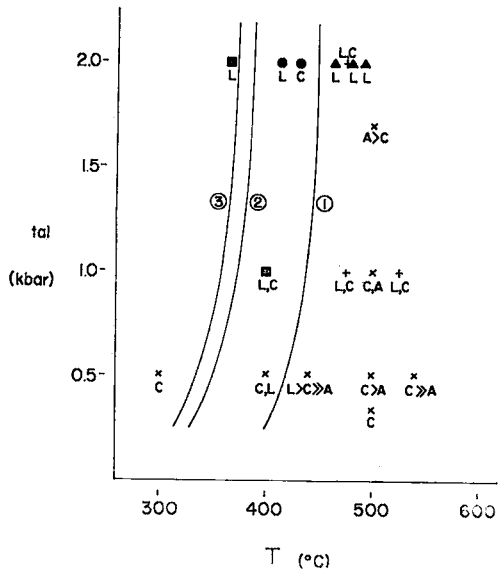

FIG. 6. Compilation of the synthesis and phase equilibrium data on the serpentine minerals as a function of temperature and pressure (L=lizardite, C=chrysotile, A=antigorite). For the composition data: x=Iishi & Saito (1973) composition fixed at $5.46Mg(OH)_2:4.0SiO_2:10.92H_2O$; • = Chernosky (1975), no Al, excess water; ■ = Chernosky (1975), Al contents vary $0.0 \leq X < 0.25$, where x is defined by $(Mg_{6-x}Al_x)(Si_{4-x}Al_x)O_{10}(OH)_8$; ▲ = Chernosky (1975), Al contents vary $0.25 \leq X \leq 2.0$; + = Page (1966), fixed composition $5.6MgO:4.0SiO_2$ with excess water. Curve 1 determined by Chernosky (1973) for the phase assemblage chrysotile, talc, forsterite, water; curve 2 determined by Johannes (1968) for the assemblage chrysotile, brucite, forsterite, water; curve 3 determined in this study for the assemblage chrysotile, brucite, magnetite, olivine (Fo_{93}), water, with oxygen fugacity defined by IM buffer.

erals from experimental studies and from the determined compositional variations in the natural phases (Whittaker & Wicks 1970) suggest that lizardite and chrysotile form in overlapping compositional ranges corresponding structurally to $b_{oct} > b_{tet}$ (Wicks & Whittaker 1975).

Either lizardite or chrysotile can form in the Al- and Fe-free system (Wicks & Whittaker 1975). Both minerals can and do form together, as observed experimentally (Page 1966; Iishi & Saito 1973; Chernosky 1975; this study) and in their occurrence in serpentinized ultramafic rocks. Wicks & Whittaker (1975) also discuss how the serpentine minerals adjust structurally to the substitution of other cations for Mg^{2+} and Si^{4+}.

The two-phase lizardite+chrysotile field was found for cation substitutions (chiefly Fe^{3+} and Al^{3+}) in the range $0 \leq x < 0.25$ (Page 1966; Chernosky 1975). Wicks & Whittaker (1975) argue on structural grounds that the two minerals are polymorphs, but the exact nature of the polymorphic relationship between lizardite and chrysotile is unknown. Their formation in nature may be a function of T,P and nucleation rate. A close crystallographic relationship exists between olivine and lizardite (Wicks 1969; Dungan 1976) indicating that replacement of olivine by lizardite occurs by a heterogenous reaction mechanism in which the oxygen anion framework of the olivine is preserved and cations migrate into and out of the structure (Brindley 1963; Wicks 1969). This topotactic relationship between olivine and lizardite may be the principle reason why lizardite forms as the first alteration mineral, followed by chrysotile. Chrysotile's chief occurrence in serpentinites is as a vein mineral or as a replacement of previously formed lizardite or antigorite. Rarely has chrysotile been observed as a direct alteration product of olivine or pyroxene. Kinetically, the nucleation and growth of lizardite occurs with relative ease compared to that of chrysotile. Increased temperature may overcome a nucleation barrier, allowing chrysotile to nucleate and grow. The experimental results at higher temperatures indicate growth of chrysotile (at the expense of lizardite?) and suggest that chrysotile is the stable polymorph relative to lizardite. However, these solid-solid reactions are extremely sluggish and the above conclusions are tentative, though petrographic textural observations tend to support experiment.

ACKNOWLEDGMENTS

This paper represents part of a dissertation submitted to McGill University in partial fulfillment of the requirements for the degree of Doctor of Philosophy. Financial support for the research was given by National Research Council of Canada Grant A-7719 to W. H. MacLean. Additional financial support was received from the Faculty of Graduate Studies and Research, McGill University, in scientific equipment grants to R. F. Martin and H. Helmstaedt, and a Sigma Xi Grant-in-Aid to Research to the author. A National Research Council of Canada Research Assistanceship from Grant A-7719, the J. P. Lynch Fellowship of McGill University and a National Research Council of Canada Post-Graduate Scholarship provided personal financial support to the author.

F. J. Wicks, Royal Ontario Museum, supplied mineral standards and through many discussions and interest in this work provided invaluable insight into serpentine mineralogy and

serpentinization. I. Barnes, U. S. Geological Survey, showed the author the classic spring localities in serpentinites of California and provided stimulating discussions in the field. D. R. Wones, U. S. Geological Survey, consistently showed interest in this study by discussion, sent the author calculations bearing on the iron-magnetite buffer and provided much encouragement with difficult experimental problems. H. R. Shaw of the U. S. Geological Survey provided important discussion on problems relating to thermochemical data and the hydrogen buffer and critically reviewed the manuscript. The kind cooperation and discussion on problems of mutual interest with O. R. Eckstrand, Geological Survey of Canada, is greatly appreciated. R. G. Hargraves and N. Dorety, Princeton University, generously performed the magnetic susceptibility measurements of some of the experimental materials. J. V. Chernosky, University of Maine, and K. Iishi, Yamaguchi University, provided preprints of their then unpublished work. S. D. Ludington, U. S. Geological Survey critically reviewed the manuscript. At McGill University, critical help and discussion was provided by: M. D. Croucher, H. Helmstaedt, S. J. Horska, W. H. MacLean, R. F. Martin, A. J. Pearce, A. Seethie and G. R. Webber.

The author deeply appreciates the financial, personal and professional support of the above individuals and institutions.

References

BAILEY, S. W. (1969): Polytypism of trioctahedral 1:1 layer silicates. *Clays Clay Minerals* **17**, 355-371.

BARNES, I. & O'NEIL, J. R. (1969): The relationship between fluids in some fresh Alpine-type ultramafics and possible modern serpentinization, Western U. S. *Geol. Soc. Amer. Bull.* **80**, 1947-1960.

———, RAPP, J. B. & O'NEIL, J. R. (1972): Metamorphic assemblages and the direction of flow of metamorphic fluids in four instances of serpentinization. *Contr. Mineral. Petrology* **35**, 263-276.

BRINDLEY, G. W. (1963): Crystallographic aspects of some decomposition and recrystallization reactions. *Proc. Ceram. Sci.* **3**, 1-55.

BURNHAM, Charles W. (1962): LCLSQ, crystallographic lattice-constant least squares refinement program. *Carnegie Inst. Wash. Year Book* **61**, 132-135.

BURNHAM, C. Wayne, HOLLOWAY, J. R. & DAVIES, N. F. (1969): Thermodynamic properties of water to 1000°C and 10,000 bars. *Geol. Soc. Amer. Spec. Pap.* **132**.

CAMERON, K. L. (1975): An experimental study of actinolite-cummingtonite phase relations with notes on the synthesis of Fe-rich anthophyllite. *Amer. Mineral.* **60**, 375-390.

CHERNOSKY, J. V. (1973): The stability of chrysotile $Mg_3Si_2O_5(OH)_4$, and the free energy of talc, $Mg_3Si_4O_{10}(OH)_4$. *Geol. Soc. Amer. Ann. Meet. Program Abstr.* **5**, 575.

——— (1975): Aggregate refractive indices and unit cell parameters of synthetic serpentine in the system MgO-Al_2O_3-SiO_2-H_2O. *Amer. Mineral.* **60**, 200-208.

DUNGAN, M. A. (1977): The petrology of bastites formed by the serpentinization of orthopyroxene, clinopyroxene and tremolitic amphibole. (In prep.)

EUGSTER, H. P. (1957): Heterogeneous reactions involving oxidation and reduction at high pressures and temperatures. *J. Chem. Phys.* **26**, 1760-1761.

——— (1959): Reduction and oxidation in metamorphism. *Researches in Geochemistry* (P. H. Abelson, ed.), 397-426. John Wiley & Sons, N. Y.

——— & WONES, D. R. (1962): Stability relations of the ferruginous biotite, annite. *J. Petrology* **3**, 82-125.

EVANS, H. T., APPLEMAN, D. E. & HANDWERKER, D. S. (1963): The least squares refinement of crystal unit cells with powder diffraction data by an automatic computer indexing method. *Abstr. Amer. Cryst. Assoc. Meet.*, Cambridge, Mass., 42-43.

FISHER, G. W. & MEDARIS, L. G. (1969): Cell dimensions and X-ray determinative curve for synthetic Mg-Fe olivines. *Amer. Mineral.* **54**, 741-753.

FORBES, W. C. (1969): Unit-cell parameters and optical properties of talc on the join $Mg_3Si_4O_{10}(OH)_2$-$Fe_3Si_4O_{10}(OH)_2$. *Amer. Mineral.* **54**, 1399-1408.

——— (1971): Iron content of talc in the system $Mg_3Si_4O_{10}(OH)_2$-$Fe_3Si_4O_{10}(OH)_2$. *J. Geol.* **79**, 63-74.

FYFE, W. S. (1973): Dehydration reactions. *Amer. Assoc. Petroleum Geol. Bull.* **57**, 190-197.

HAAS, J. L. & ROBIE, R. A. (1973): Thermodynamic data for wustite $Fe_{0.947}O$, magnetite Fe_3O_4, and hematite Fe_2O_3. *Trans. Amer. Geophys. Union* **54**, 483 (Abstr.).

HOSTETLER, P. B., COLEMAN, R. G., MUMPTON, F. A. & EVANS, B. W. (1966): Brucite in Alpine serpentinites. *Amer. Mineral.* **51**, 75-98.

HUEBNER, J. S. (1971): Buffering techniques for hydrostatic systems at elevated pressures. *In* Research Techniques for High Pressure and High Temperatures (G. C. Ulmer, ed.), 123-177. Springer-Verlag, N. Y.

IISHI, K. & SAITO, M. (1973): Synthesis of antigorite. *Amer. Mineral.* **58**, 915-919.

JAMBOR, J. L. & SMITH, C. H. (1964): Olivine composition determination with small diameter X-ray powder cameras. *Mineral. Mag.* **33**, 730-741.

JOHANNES, W. (1968): Experimental investigation of the reaction forsterite + H_2O = serpentine + brucite. *Contr. Mineral. Petrology* **19**, 309-315.

——— (1969): An experimental investigation of the system MgO-SiO_2-H_2O-CO_2. *Amer. J. Sci.* **267**, 1083-1104.

KHEIKER, D. M., FLANTSBAUM, I. M. & BUBELEVA, L. V. (1967): Determination of elementary fiber

dimensions in chrysotile asbestos. *Soviet Phys. Cryst.* **12**, 370-374.

KORYTKOVA, E. N. & MAKAROVA, T. A. (1971): Experimental study of the serpentinization of olivine. *Dokl. Akad. Nauk U.S.S.R.* **196**, 144-145.

———, ——— & KOSULINA, G. I. (1972): Experimental serpentinization of olivine. *Int. Geol. Rev.* **14**, 1074-1078.

KRSTANOVIC, I. (1968): Crystal structure of single-layer lizardite. *Z. Krist.* **126**, 163-169.

KUBASCHEWSKI, O. & VON GOLDBECK, O. (1949): The thermodynamics of the iron nickel alloys. *Trans. Faraday Soc.* **45**, 948-960.

KULLERUD, G. (1971): Experimental techniques in dry sulfide research. *In* Research Techniques for High Pressure and High Temperature (G. C. Ulmer, ed), 289-315. Springer-Verlag, New York.

LONEY, R. A., HIMMELBERG, G. R. & COLEMAN, R. G. (1971): Structure and petrology of the Alpine type peridotite at Burro Mountain, California, U.S.A. *J. Petrology* **12**, 245-309.

MARTIN, B. & FYFE, W. S. (1970): Some experimental and theoretical observations of kinetics of hydration reactions with particular reference to serpentinization. *Chem. Geol.* **6**, 185-202.

MIYASHIRO, A. (1966): Some aspects of peridotite and serpentinite in orogenic belts. *J. Geol. Geophys. Japan* **37**, 45-61.

MOODY, J. B. (1974): *Serpentinization of Iron-Bearing Olivines: An Experimental Study*. Ph.D. thesis, McGill Univ.

MUMPTON, F. A. & THOMPSON, C. S. (1966): The stability of brucite in the weathering zone of the New Idria serpentinite. *Clays Clay Minerals, Proc. 14th Nat. Conf.*, 249-257. Pergamon Press, New York.

PAGE, N. J (1966): *Mineralogy and Chemistry of the Serpentine Group Minerals and the Serpentinization Process*. Ph.D. thesis, Univ. Calif., Berkeley.

——— (1967): Serpentinization at Burro Mountain, Calif. *Contr. Mineral. Petrology* **14**, 321-342.

ROBIE, R. A. & WALDBAUM, D. R. (1968): Thermodynamic properties of minerals and related substances at 298.15°K (25.0°C) and one atmosphere (1.013 bars) pressure and at higher temperatures. *U. S. Geol. Surv. Bull.* **1259**.

ROSS, M. (1968): X-ray diffraction effects by non-ideal crystals of biotite, muscovite, montmorillonite mixed-layer clays, graphite and periclase. *Z. Krist.* **126**, 80-97.

SCARFE, C. M. & WYLLIE, P. J. (1967): Serpentine dehydration curves and their bearing on serpentine deformation in orogensis. *Nature* **215**, 945-946.

SHAW, H. R. (1967): Hydrogen osmosis in hydrothermal experiments. *In* Researches in Geochemistry 2 (P. H. Abelson, ed.), 521-541. John Wiley & Sons, N. Y.

——— & WONES D. R. (1964): Fugacity coefficients for hydrogen gas between 0°C and 1000°C for pressures to 3000 atm. *Amer. J. Sci.* **262**, 918-929.

TUTTLE, O. F. (1949): Two pressure vessels for silicate-water studies. *Geol. Soc. Amer. Bull.* **60**, 1727-1729.

WHITTAKER, E. J. W. (1957): The structure of chrysotile. V. Diffuse reflections and fiber texture. *Acta Cryst.* **10**, 149.

——— & WICKS F. J. (1970): Chemical differences among the serpentine polymorphs: a discussion. *Amer. Mineral.* **55**, 1025-1047.

——— & ZUSSMAN, J. (1956): The characterization of the serpentine minerals by X-ray diffraction. *Mineral. Mag.* **31**, 107-126.

WICKS, F. J. (1969): *X-ray and Optical Studies on Serpentine Minerals*. D. Phil. thesis, Oxford Univ.

——— & WHITTAKER, F. J. W. (1975): A reappraisal of the structures of the serpentine minerals. *Can. Mineral.* **13**, 227-243.

WISE, W. S. & EUGSTER, H. P. (1964): Celadonite: synthesis, thermal stability and occurrence. *Amer. Mineral.* **49**, 1031-1083.

WONES, D. R. & EUGSTER, H. P. (1965): Stability of biotite: experiment, theory and application. *Amer. Mineral.* **50**, 1228-1272.

YADA, J. C. (1967): Study of chrysotile asbestos by a high resolution electron microscope. *Acta Cryst.* **23**, 704-707.

——— (1971): Study of microstructure of chrysotile asbestos by high resolution electron microscopy. *Acta Cryst.* **27A**, 659-664.

ZEN, E. (1973): Thermochemical parameters of minerals from oxygen-buffered hydrothermal equilibrium data, method, application to annite and almandine. *Contr. Mineral. Petrology* **39**, 65-80.

ZUSSMAN, J., BRINDLEY, G. W. & COMER, J. J. (1957): Electron diffraction studies of serpentine minerals. *Amer. Mineral.* **42**, 133-153.

ZVYAGIN, B. B. (1967): *Electron-Diffraction Analysis of Clay Mineral Structures*. Plenum Press, New York.

Manuscript received December 1975, emended May 1976.

APPENDIX 1. HYDROTHERMAL RUN TABLE

Run	Starting Material	T(°C)	P(kbar)	Run Duration hrs	Buffer	Fluid*	Products**
			Experiments with synthetic and natural olivines + pure water				
3-14	0 (2-17)	376	1.94	1128	IM	water	O
3-60	0 (2-17)	338	1.94	674	IM	water	maj. O, L, C, tr. B, M
3-25	0 (2-17)	323	1.94	742	IM	water	min. O, L, tr. C, B, M
3-15	0 (2-17)	349	1.99	1107	IM	water	maj. O, L, M
3-26	0 (2-17)	322	1.94	739	IM	water	tr. O, L, B, M
3-12	0 (2-17)	321	1.99	1150	IM	water	tr. O, L, C, B, M
3-61	0 (2-17)	302	1.93	504	IM	water	tr. O, L, C, B, M
2-95	0 (2-33)	375	1.47	504	IM	water	O
2-92	0 (2-19)	351	1.47	576	-	water	tr. O, L, C, B
2-94	0 (2-33)	339	1.47	575	IM	water	min. O, L, tr. B, M
2-99	0 (2-33)	329	1.47	529	IM	water	tr. O, L, C, M
3-30	0 (OP-194)	331	1.47	764	IM	water	maj. O, L, C. tr. B, M
3-48	0 (GSC)	309	1.48	1773	IM	water	tr. O, L, C, B, M
3-32	0 (GSC)	307	1.47	911	IM	water	min. O, L, B, M
2-98	0 (2-33)	302	1.47	625	IM	water	tr. O, L, C, B, M
3-5	0 (2-17)	376	1.00	1539	IM	water	O, tr. L
3-3	0 (2-17)	349	1.01	1559	IM	water	O, tr. L, tr. B
3-31	0 (OP-54)	321	0.99	764	IM	water	?
3-2	0 (2-17)	329	1.01	1637	IM	water	O, tr. L
3-4	0 (2-17)	317	1.01	1492	IM	water	tr. O, L, C, B, M
3-1	0 (2-17)	302	1.01	1660	IM	water	tr. O, L, C, B, M
2-109	0 (2-33)	377	0.51	720	IM	water	O
2-108	0 (2-33)	349	0.51	793	IM	water	min. O, L, B, M
3-23	0 (2-17)	323	0.54	1606	IM	water	maj. O, L, M, C
2-110	0 (2-33)	316	0.51	743	IM	water	min. O, L, C, B, M
3-22	0 (2-17)	304	0.54	1605	IM	water	tr. O, L, C, B, M
3-77	2-BU-77	307	1.93	999	IM	water	tr. O, L, C, B, M
2-101	M7863	375	1.47	504	IM	water	O
2-100	M7863	347	1.47	528	IM	water	maj. O, L, C, B, M
2-107	M7863	328	1.47	819	IM	water	min. O, L, C, B, M
2-102	M7863	317	1.47	504	IM	water	min. O, L, C, B, M
2-106	M7863	303	1.47	815	IM	water	maj. O, L, B, M
3-47	M7863	331	1.00	1127	IM	water	min. O, L, B, M
			Experiments with synthetic and natural olivines with fluids of variable composition				
3-50	0 (2-17)	352	1.48	525	IM	0.14 M $NaSi^+$	min. O, L, C, tr. M, (?)
3-51	0 (2-17)	317	1.48	525	IM	0.12 M $NaSi^+$	tr. O, L, M
3-43	0 (2-17)	331	0.99	573	IM	0.05 M $NaSi^+$	min. O, L, M
3-42	0 (2-17)	306	0.99	573	IM	0.06 M $NaSi^+$	L, C, B, M
3-62	0 (2-17)	372	1.00	517	IM	0.39 M NaCl	O, tr. L, tr. B, tr. M
3-56	0 (2-17)	351	1.00	481	IM	0.14 M NaCl	O, tr. L, M
3-55	0 (2-17)	319	1.00	481	IM	0.12 M NaCl	O, L, M
3-57	0 (2-17)	300	1.00	483	IM	0.25 M NaCl	O, tr. L, M
3-45	0 (2-17)	355	0.99	524	IM	0.01 M NaOH	O, tr. L, M, tr. B
3-49	0 (2-17)	342	1.48	596	IM	0.03 M NaOH	min. O, L, tr. C, M, B
3-46	0 (2-17)	322	1.48	524	IM	0.01 M NaOH	tr. O, L, B, M, tr. C
3-54	0 (2-17)	302	1.00	550	IM	0.01 M NaOH	tr. O, L, C, B, M
3-63	0 (2-17)	332	1.00	525	IM	0.19 M NaCl 0.01 M NaOH	O, tr. L, tr. B
3-64	0 (2-17)	302	1.00	524	IM	0.33 M NaCl 0.02 M NaOH	tr. O, L, C, B, M
3-96	2-BU-66	346	2.01	433	IM	0.23 M NaCl 0.01 M NaOH	O, L, C, B, M
3-95	2-BU-66	330	2.01	433	IM	0.23 M NaCl 0.01 M NaOH	min. O, L, C, B, M
3-92	2-BU-66	317	1.00	526	IM	0.12 M NaCl 0.01 M NaOH	min. O, L, C, B, M
3-93	2-BU-66	320	0.57	479	IM	0.19 M NaCl 0.01 M NaOH	tr. O, L, C, B, M
3-94	2-BU-66	310	0.57	478	IM	0.12 M NaCl 0.01 M NaOH	min. O, L, C, B, M
			Reversed experiments on the reaction boundary for olivine (Fo_{93}) + H_2O				
3-101	equil mix++	392	2.02	695	IM	water	O, L, C, B, tr. M
3-100	equil mix	376	2.01	794	IM	water	O, L, C, B, M
3-99	equil mix	361	2.01	793	IM	water	O, L, C, B, M
3-76	equil mix	344	1.93	479	IM	water	tr. O, L, C, B, M
3-75	equil mix	335	1.93	480	IM	water	tr. O, L, C, B, M
3-74	equil mix	341	1.48	481	IM	water	tr. O, L, C, B, M
3-72	equil mix	332	1.48	791	IM	water	tr. O, L, C, B, M
3-86	equil mix	371	1.01	569	IM	water	O, L, C, B, tr. M
3-87	equil mix	361	1.01	568	IM	water	O, L, C, B, tr. M
3-85	equil mix	349	1.01	567	IM	water	O, L, C, B, M
3-84	equil mix	341	1.01	568	IM	water	O, L, C, B, M
3-71	equil mix	330	1.00	792	IM	water	tr. O, L, C, B, M
3-78	equil mix	321	1.01	384	IM	water	tr. O, L, C, B, M
3-70	equil mix	322	1.00	837	IM	water	tr. O, L, C, B, M
3-98	equil mix	352	0.54	814	IM	water	O, L, C, B, M
3-97	equil mix	336	0.54	814	IM	water	O, L, C, B, M
3-68	equil mix	322	0.56	863	IM	water	tr. O, L, C, B, M
3-69	equil mix	311	0.56	895	IM	water	tr. O, L, C, B, M

Appendix I (continued)

Dehydration reactions

3-106	3-77	370	2.01	1014	IM	water	tr. O, L, C, B, M
3-105	3-77	355	2.01	1014	IM	water	tr. O, L, C, B, M
3-103	3-77	356	1.01	1035	IM	water	tr. O, L, C, B, M
3-102	3-77	339	1.01	1058	IM	water	tr. O, L, C, B, M
3-104	3-77	330	1.01	1035	IM	water	tr. O, L, C, B, M

tr. = trace amount present <2% O = olivine C = chrysotile M = magnetite
min. = minor amount present 2-40% L = lizardite B = brucite IM = iron-magnetite
maj. = major amount present >40%
Run duration was measured from the time the bomb was placed in furnace; all runs were brought to temperature and quenched isobarically.

*initial fluid composition

**% olivine is an approximate volume estimate from optical and X-ray results, % magnetite is estimated from polished section

+sodium metasilicate, $Na_2SiO_3.9H_2O$

++a mixture composed of equal weights of products of Run 3-48 + GSC olivine

APPENDIX 2a. X-RAY POWDER DIFFRACTION DATA FOR LIZARDITE

	M19804, 1T			3-61			3-4			3-97			3-76		
hkl	$d_{(calc)}$	$d_{(obs)}$	I*	$d_{(calc)}$	$d_{(obs)}$	I*	$d_{(calc)}$	$d_{(obs)}$	I*	$d_{(calc)}$	$d_{(obs)}$	I**	$d_{(calc)}$	$d_{(obs)}$	I**
001	7.313	7.332	10	7.291	7.272	10	7.298	7.302	10	7.300	7.332	100	7.292	7.296	100
020	4.611	4.614	2	4.598	4.590	3	4.589	4.585	3	4.599	4.595	42	4.598	4.595	46
021	3.900	3.900	2							3.891	3.888	53	3.889	3.886	100
002	3.656	3.658	3	3.645	3.646	7	3.649	3.650	8	3.650	3.655	78	3.646	3.649	52
200	2.659	2.659	2												
201	2.501	2.499	6	2.496	2.493	6	2.491	2.495	4	2.496	2.514	78	2.495	2.514	27
202	2.151	2.149	3												
206	1.797	1.795	2	1.795	1.795	6	1.793	1.793	6	1.794	1.793	42	1.794	1.794	25
028	1.694	1.700	3	1.695	1.702	4				1.692	1.699	48	1.694	1.701	23
060	1.537	1.536	7	1.532	1.535	5	1.529	1.535	4	1.533	1.535	50	1.532	1.536	29
204	1.504	1.504	3	1.499	1.500	5	1.497	1.497	3	1.500	1.499	43	1.499	1.500	48
401	1.308	1.308	3												
402	1.293	1.293	2												

* estimated visually

** microdensitometer measurements

Samples 3-61 and 3-4 were massive, anhedral lizardite; 3-97 and 3-76 were platy and euhedral lizardite.

APPENDIX 2b. X-RAY POWDER DIFFRACTION DATA FOR CHRYSOTILE

	M8507, $2M_{cl}$			3-48			3-42			3-64			3-105		
hkl	$d_{(calc)}$	$d_{(obs)}$	I*	$d_{(calc)}$	$d_{(obs)}$	I	$d_{(calc)}$	$d_{(obs)}$	I	$d_{(calc)}$	$d_{(obs)}$	I	$d_{(calc)}$	$d_{(obs)}$	I
002	7.303	7.302	10	7.305	7.292	10	7.312	7.350	10	7.301	7.314	10	7.320	7.320	10
020	4.604	4.585	4	4.607	4.590	3	4.606	4.571	6	4.600	4.583	4	4.606	4.595	3
004	3.651	3.652	8												
130	2.651	2.655	3				2.657	2.657	5	2.654	2.655	2			
201	2.586	2.587	2												
$20\bar{2}$	2.543	2.543	3				2.532	2.529	8	2.532	2.531	6			
202	2.451	2.452	8	2.433	2.457	3	2.452	2.453	8	2.450	2.452	7	2.446	2.458	4
203	2.227	2.276	1	2.269	2.271	2							2.270	2.270	5
$20\bar{4}$	2.209	2.209	1												
204	2.091	2.091	6	2.091	2.089	2	2.096	2.094	7	2.094	2.093	4			
206	1.745	1.763	3	1.751	1.750	2	1.738	1.741	5	1.737	1.746	2	1.738	1.751	3
060	1.534	1.535	3	1.535	1.535	5	1.535	1.535	7	1.533	1.534	4	1.535	1.535	5
$40\bar{2}$	1.293	1.319	2	1.316	1.317	4				1.313	1.315	3	1.308	1.316	5

*estimated visually